AGU PUBLICATIONS

Geophysical Research Letters

RESEARCH LETTER
10.1002/2013GL059010

Key Points:
- Dynamic mass loss is mostly controlled by <10% of fast-flowing outlet glaciers
- Dynamic acceleration and thinning cause brief, asynchronous discharge increases
- Changes in surface mass balance not discharge will drive future sea level rise

Supporting Information:
- Readme
- Figure S1
- Figure S2
- Figure S3
- Figure S4
- Figure S5

Correspondence to:
E. M. Enderlin,
ellyn.enderlin@gmail.com

Citation:
Enderlin, E. M., I. M. Howat, S. Jeong, M.-J. Noh, J. H. van Angelen, and M. R. van den Broeke (2014), An improved mass budget for the Greenland ice sheet, *Geophys. Res. Lett.*, *41*, 866–872, doi:10.1002/2013GL059010.

Received 11 DEC 2013
Accepted 10 JAN 2014
Accepted article online 16 JAN 2014
Published online 7 FEB 2014

An improved mass budget for the Greenland ice sheet

Ellyn M. Enderlin[1,2,3], Ian M. Howat[1,2], Seongsu Jeong[1,2], Myoung-Jong Noh[1], Jan H. van Angelen[4], and Michiel R. van den Broeke[4]

[1]Byrd Polar Research Center, Ohio State University, Columbus, Ohio, USA, [2]School of Earth Sciences, Ohio State University, Columbus, Ohio, USA, [3]Now at Climate Change Institute, University of Maine, Orono, Maine, USA, [4]Institute for Marine and Atmospheric Research, Utrecht University, Utrecht, Netherlands

Abstract Extensive ice thickness surveys by NASA's Operation IceBridge enable over a decade of ice discharge measurements at high precision for the majority of Greenland's marine-terminating outlet glaciers, prompting a reassessment of the temporal and spatial distribution of glacier change. Annual measurements for 178 outlet glaciers reveal that, despite widespread acceleration, only 15 glaciers accounted for 77% of the 739 ± 29 Gt of ice lost due to acceleration since 2000 and four accounted for ~50%. Among the top sources of loss are several glaciers that have received little scientific attention. The relative contribution of ice discharge to total loss decreased from 58% before 2005 to 32% between 2009 and 2012. As such, 84% of the increase in mass loss after 2009 was due to increased surface runoff. These observations support recent model projections that surface mass balance, rather than ice dynamics, will dominate the ice sheet's contribution to 21st century sea level rise.

1. Introduction

The Greenland ice sheet (GrIS) is losing mass as a result of both increased surface melting and runoff and increased ice discharge from marine-terminating outlet glaciers [*Rignot et al*., 2008, 2011; *Sasgen et al*., 2012; *van den Broeke et al*., 2009]. The contribution of these two processes to total ice sheet loss was approximately equal during the first decade of the 21st century [*van den Broeke et al*., 2009], a period of both rapid warming [*Hanna et al*., 2012] and widespread retreat and acceleration of marine-terminating outlet glaciers [*Howat et al*., 2008; *Joughin et al*., 2010; *McFadden et al*., 2011; *Moon and Joughin*, 2008; *Moon et al*., 2012; *Walsh et al*., 2012], with the latter linked to changes in coastal ocean circulation [*Holland et al*., 2008; *Seale et al*., 2011; *Straneo et al*., 2012]. In a study published soon after synchronous ice flow acceleration was detected in southeast Greenland, *Pfeffer et al*. [2008] provided a kinematic, upper bound estimate of the potential contribution of Greenland ice discharge to sea level rise over the next century assuming the rapid, widespread, and sustained acceleration of Greenland's marine-terminating outlet glaciers. More recent observations, however, indicate a substantially smaller maximum acceleration than postulated in the *Pfeffer et al*. [2008] estimates [*Moon et al*., 2012], and numerical flow models, based on the few glaciers with sufficient data, predict a far smaller contribution to sea level rise from ice dynamic change than from surface melting and runoff [*Goelzer et al*., 2013; *Nick et al*., 2013; *Price et al*., 2011].

Changes in the total discharge from the ice sheet are the summation of changes in ice flow from individual outlet glaciers in response to a complex, and poorly understood, interaction between atmospheric and oceanographic forcing and ice flow dynamics [*Straneo et al*., 2013; *Joughin et al*., 2012]. Until recently, thickness data only existed for a small number of outlet glaciers, so that estimates of total discharge required the extrapolation of thickness data from the ice sheet interior or interpolations through time [*Rignot et al*., 2008, 2011; *van den Broeke et al*., 2009], imparting large uncertainties and preventing a complete assessment of temporal and spatial variability of discharge at the scale of individual outlet glaciers.

As a result of the NASA Operation IceBridge ice-penetrating radar surveys conducted by the Center for Remote Sensing of Ice Sheets (CReSIS) at the University of Kansas, ice thickness measurements have dramatically improved in coverage and quality over the past few years, enabling measurements of discharge at the scale of individual outlet glaciers, rather than ice catchments. These capabilities have been demonstrated for three of Greenland's largest and best observed outlet glaciers (Jakobshavn Isbræ, Kangerdlugssuaq, and Helheim) for which monthly mass budgets were derived between 2000 and 2010 [*Howat et al*., 2011]. Here we extend this method to construct annual discharge time series for 178 marine-terminating outlet glaciers with termini wider than 1 km (Figure S1). Using these high-resolution time series, we assess the contribution of individual outlet glaciers to ice sheet discharge and cumulative discharge change. These data are also used to assess the recent contribution of glacier discharge to ice sheet mass loss and to provide a kinematic constraint on the contribution of ice dynamic change to 21st century sea level rise.

2. Data and Methodology

Of the 178 marine-terminating glaciers with termini wider than 1 km, 81 glaciers had ice thickness transects across their trunks, allowing for complete discharge calculations (Figure S1). These include all but one glacier wider than 9 km (Storstrommen). For 37 glaciers, ice thickness measurements were only available along the axis of flow, so that discharge estimates required an assumption of the relationship between glacier width at the surface and cross-sectional area. All but six glaciers wider than 5 km had cross-sectional or flow line thickness measurements. The remaining 60 glaciers had no thickness measurements (Figure S1). The south, southeast, and Giesecke Peninsula (including the Geikie Plateau) had the largest number of unsurveyed glaciers, whereas nearly all glaciers along the northwest coast had bed transect data (Figure S1).

For glaciers with across-flow thickness transects (i.e., gates), we selected the survey up glacier of, and closest to, the grounding line and extracted surface speed and thickness data along the transect. We observed surface speeds south of ~81°N latitude using repeat-image feature tracking as described in *Howat et al*. [2011], utilizing orthorectified imagery from the Landsat 7 Enhanced Thematic Mapper Plus and the Advanced Spaceborne Thermal and Reflectance Radiometer (ASTER). As in previous studies, we assumed that speed is constant with depth for these fast-flowing ($>$ 1 km/a) glaciers, where nearly all motion is at the base. Thickness was calculated by subtracting the bed elevation from the surface elevation for each year. Surface elevations were obtained from orthorectified ASTER digital elevation models (DEMs) produced by the Land Processes Distributed Active Archive Center and SPOT5 DEMs produced by the SPOT 5 stereoscopic survey of Polar Ice: Reference Images and Topographies (SPIRIT) program [*Korona et al*., 2009] as well as NASA Airborne Topographic Mapper lidar measurements. We filtered the elevation and speed data using an adaptive median filter and calculated annual median speeds and elevations.

Using these observations, we calculated ice discharge as the summed product of ice density, ρ_i, surface speed, U, thickness, H, and distance between survey points dy across the flux gates of width W. Since the fluxgates are located within 5 km of the grounding line, the volume of surface melt runoff seaward of the fluxgate is negligible, and the flux across the fluxgate was assumed to equal to the discharge. The error in discharge at each point across the flux gate consists of spatially random, σ, and systematic (bias) components, μ, given by

$$D_\sigma = D\sqrt{\left(\frac{U_\sigma}{U}\right)^2 + \left(\frac{H_\sigma}{H}\right)^2} \tag{1}$$

$$D_\mu = D\sqrt{\left(\frac{U_\mu}{U}\right)^2 + \left(\frac{H_\mu}{H}\right)^2}, \tag{2}$$

with the total error summing to

$$D_e = \sum_0^W D_\mu + \sqrt{\sum_0^W D_\sigma^2}. \tag{3}$$

Systematic errors are expected to dominate for both speed and thickness observations. Here we present all errors as 1 standard deviation (i.e., ±1σ). In the case of speed, random errors are due to pixel matching ambiguities and are on the order of 20 m/a while systematic errors in coregistration between image pairs are typically 200 m/a [*Ahn and Howat*, 2011]. For ice thickness, random errors are mostly due to errors in the DEMs, which are coregistered to have zero bias, and are typically 5 m [*Noh and Howat*, 2013] while systematic errors arise from the location of the bed elevation, with an uncertainty of ±20 m. We note that since the bed elevation is assumed constant in time, this is the only error that is also systematic in time. Discharge error for fluxgate solutions averaged ±0.43 Gt/a, or ±22%, over the entire sample and less than 10% for glaciers with discharge 1 Gt/a or greater.

For glaciers with only flow line bed elevation data, we segmented the flight line into a 2 km section, approximately 5 km above the ice front/grounding line. We then sampled and filtered speed and elevation data at the transect location and took the mean values over the section to use in the discharge calculation. Since only glacier width at the surface is known, we multiply the surface width by a shape factor, *sf*, to estimate an effective width that accounts for cross-sectional area [*Howat et al*., 2011]. Based on glaciers with surveyed fluxgates, we obtain a mean and standard deviation for *sf* of 0.5 ± 0.16. Error in discharge from centerline data is then

$$D_e = D\sqrt{\left(\frac{\overline{W}_e}{\overline{W}}\right)^2 + \left(\frac{U_e}{U}\right)^2 + \left(\frac{H_e}{H}\right)^2}, \quad (4)$$

where the subscript, *e*, is the total error. Due to the added uncertainty introduced by the parameterization of cross-sectional area, compared to fluxgate estimates, errors are several times larger for discharges derived from centerline measurements, averaging ±0.79 Gt/a for the entire sample, or ±33% for glaciers with discharges greater that 1 Gt/a.

Discharge was estimated for glaciers with no bed data using the empirical relationship between the product of width and centerline speed and discharge at surveyed glaciers with ice thickness observations. As shown in Figure S2, discharge shows a strongly significant correlation ($r^2 = 0.62$) with the product of width and centerline speed. Using the linear least squares fit between these variables, and its 95% confidence interval, discharge and errors were predicted at unsurveyed glaciers using their width and centerline speed. The average uncertainty in discharge for glaciers without bed data is 0.75 Gt/a or ±36% for glaciers with discharges greater than 1 Gt/a.

We assume that errors in discharge are uncorrelated between individual glaciers, so that the error in total ice discharge is given by $\sqrt{\Sigma D_e^2}$. Errors for individual glacier discharge measurements average between ±0.35 and ±0.59 Gt/a, giving errors in total discharge of ±4.8 to ±8 Gt/a or 1 to 1.5% of the ice sheet discharge. If errors were systematic, the discharge uncertainty range would be 15 to 20% of the ice sheet discharge. The ice density, ρ_i, also carries an uncertainty of ~1% [*Cuffey and Paterson*, 2010], but it is unclear whether this uncertainty is random or systematic and is, therefore, excluded from the errors provided. Data used in our analysis are available at http://bprc.osu.edu/GDG/data.php.

3. Results

For the 118 glaciers with bed data, we find a total discharge of 389 ± 5 Gt/a for the year 2000. For the glaciers without bed data, we estimate an additional 65 ± 4 Gt/a. The four glacier catchments north of our speed data coverage contribute another 8 ± 1 Gt/a [*Rignot et al*., 2008] (catchments 2, 3, 4, and 4b), giving a total ice sheet discharge in 2000 of 462 ± 6 Gt. This estimate is within the error of the 445 ± 15 Gt/a estimated by *Rignot et al*. [2008] but is ~16% less than estimated in *Rignot et al*. [2011]. The cause of the difference in these estimates is unclear but may be due to differences in data availability and assumptions used for filling gaps (E. Rignot, personal communication, 2013) or due to differences in the method used to correct for surface mass balance between the inland fluxgates and the grounding lines. The 11 km resolution surface mass balance model used in the 2011 study may have overestimated accumulation between the fluxgates and the grounding lines over steep margins, such as in the southeast and northwest, resulting in an overprediction of the ice sheet discharge.

We find that 15 glaciers account for over 50% of the ice sheet discharge, with five accounting for over 30% (Figure S3). It is notable that Helheim Glacier is often cited as among Greenland's three largest glaciers (with Jakobshavn Isbræ and Kangerdlugssuaq) and has, accordingly, been well studied. Our data reveal, however, that Helheim is actually the fifth largest by discharge behind the much less studied Koge Bugt (second) and Ikertivaq South (fourth), both on the southeast coast. Based on this observation, these glaciers should be targeted for more detailed observation and modeling studies.

The annual time series of ice sheet discharge is shown in Figure 1. Discharge increased linearly by 17% between 2000 and 2005, reaching 542 ± 7 Gt/a. Discharge then decreased in 2006 and remained nearly constant until 2010, when it increased to a new high of 546 ± 11 Gt/a. Discharge then stabilized in 2011 and 2012 at ~19% above the 2000 value. Together, glaciers in the southeast and northwest sectors of the ice sheet

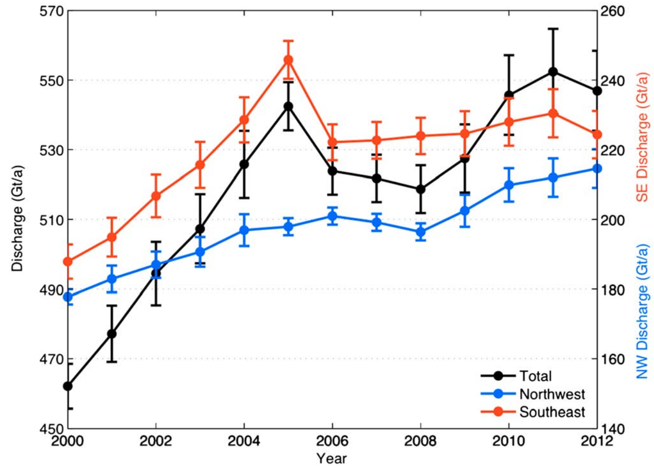

Figure 1. (left axis) The black curve is the ice sheet discharge time series and (right axis) blue and red curves are the discharge time series from the northwestern and southeastern regions, respectively. Error bars indicate the uncertainty in the annual discharge estimates.

represent 80% of the ice sheet discharge and account for 86% of the change. Figure 1 reveals that variations in total ice sheet discharge were the combination of contrasting patterns of change in these two regions. The initial increase before 2005 was mostly (72%) due to increases in the southeast, with a smaller increase in the northwest. The majority (64%) of the increase in discharge after 2008, however, was due to acceleration in the northwest, as the southeast has remained stable following the 2006 decrease in discharge from the region. The steady increase in discharge after 2000 in the northwest contradicts previous reports, based on indirect geophysical evidence, suggesting the discharge did not increase there until after 2005 [*Khan et al*., 2010; *Kjaer et al*., 2012].

To assess mass change due to variations in discharge, for each glacier we calculate the cumulative discharge anomaly as $\delta D_{\mathrm{cum},}=\Sigma(D\text{-}D_0)$, where D and D_0 are the annual and reference discharges, respectively. Thus, a positive δD_{cum} is the total ice lost due to acceleration over the observation period. Using the 2000 values for D_0 gives a total δD_{cum} of 739 ± 29 Gt by 2012, with 35% and 56% of this loss from glaciers in the northwest and southeast, respectively. Increased discharge from 15 glaciers accounted for 77% of δD_{cum} (Figure 2), with just four glaciers (Jakobshavn Isbræ, Kangerdlugssuaq, Koge Bugt, and Ikertivaq South) representing half. Out of all surveyed glaciers, 29 had cumulative discharge anomalies >5 Gt and 56 had anomalies >2 Gt, which is close to the resolvable change. An additional 53 had negative anomalies (positive mass contribution), with 12

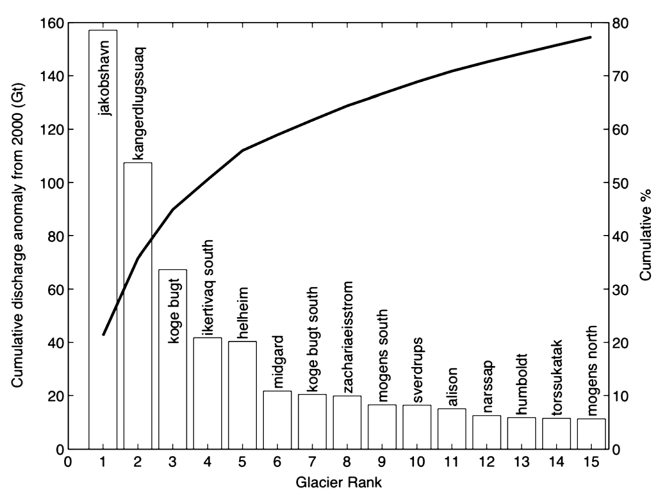

Figure 2. (left axis) The bars indicate the cumulative discharge anomaly from 2000 for the 15 glaciers with the largest contribution to mass loss and (right axis) the curve is the cumulative percentage contribution to the ice sheet's discharge anomaly.

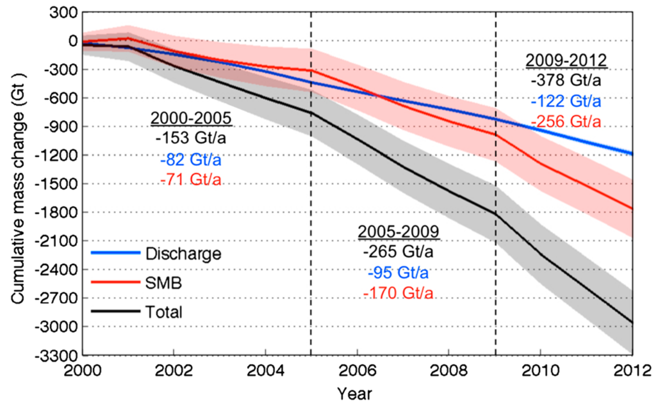

Figure 3. (black) Cumulative mass change due to (blue) discharge change with respect to 1996 and (red) surface mass balance change with respect to the 1961–1990 mean. Shading indicates uncertainty. Discharge uncertainty is shown but is visually indistinguishable. Text indicates the trend in the (black) total mass loss rate, (blue) discharge, and (red) surface mass balance during the 2000–2005, 2005–2009, and 2009–2012 periods.

having negative cumulative anomalies < -2 Gt. All glaciers with negative anomalies were located on the northwestern and southern coasts (Figure S4). In total, glaciers with negative anomalies offset loss by 85 ± 4 Gt or 12%.

To estimate total ice sheet mass change and the relative contributions of discharge and surface mass balance (SMB), we combine our discharge time series with SMB from the Regional Atmospheric Climate Model for the Greenland Ice Sheet (RACMO2/GR), which was recently upgraded with drifting snow and grain size-dependent albedo schemes. Results from the current RACMO2/GR model are described in *van Angelen et al*. [2013]. We calculate annual mass change as the deviation from a long-term steady state, typically assumed to be the 1961–1990 mean SMB of 409 ± 70 Gt/a [*Rignot et al*., 2008, 2011; *Sasgen et al*., 2012; *van den Broeke et al*., 2009]. If we account for the estimated 35 Gt/a increase in discharge observed between 1996 and 2000 [*Rignot et al*., 2008], this reference SMB is consistent with the estimated 1996 discharge (~427 Gt/a), when the ice sheet mass balance appears to have been close to equilibrium [*Zwally et al*., 2005]. We do not include volume loss due to grounding line retreat in our mass loss calculations because its contribution is negligible to the ice sheet total [*Howat et al*., 2011; *Rignot et al*., 2011].

We estimate a total mass loss between 2000 and 2012 of 2963 ± 335 Gt. Our results agree to within the uncertainty of contemporaneous estimates from Gravity Recovery and Climate Experiment (GRACE) [*Sasgen et al*., 2012; *Wouters et al*., 2013]. The rate of loss increased from 153 ± 33 Gt/a over the period 2000–2005 to 265 ± 18 Gt/a from 2005 to 2009 and 378 ± 50 Gt/a between 2009 and 2012, giving a total acceleration of 27.0 ± 9.0 Gt/a^2 since 2000. This acceleration is in good agreement with the 2003–2012 acceleration of 25 ± 9 Gt/a^2 detected by GRACE [*Wouters et al*., 2013]. The inclusion of the persistent and strongly negative SMB anomaly that occurred from 2010 through 2012 resulted in an apparent increase in mass loss acceleration relative to an earlier estimate of 17.0 ± 9.0 Gt/a^2 for the 2003–2010 period [*Rignot et al*., 2011], demonstrating the high sensitivity of derived mass loss trends to interannual mass budget variability.

4. Discussion and Conclusions

A major challenge for numerical ice sheet models has been the treatment of the large number of outlet glaciers. Modeling efforts have typically focused on those glaciers with the best observational records for constraint. *Nick et al*. [2013] used a numerical ice flow model to predict the 21st century dynamic change at four large and relatively well-studied outlet glaciers (Jakobshavn Isbræ, Helheim, Petermann, and Kangerdlugssuaq) and then derived a loss estimate for the total ice sheet by scaling up their total discharge by a factor of 5 because these glaciers drain ~1/5 of the ice sheet by area. We measure a 2000–2012 cumulative loss of 309 Gt for these five glaciers, representing 42% of the ice sheet discharge change from 2000 to 2012. Scaling by a factor of 5, therefore, overpredicts the mass loss by more than a factor of 2. This discrepancy reflects the fact that loss, as revealed by our data, is dominated by a relatively small number of glaciers, so that the contribution to loss is not necessarily proportional to drainage area. Our data set provides guidance for future observation gathering and modeling activities to provide a more representative sampling of mass change.

Our results confirm a decline in the relative importance of discharge to ice sheet mass loss (Figure 3). The 17% increase in discharge between 2000 and 2005 accounted for 58% of the mass loss during that time. This fraction decreased to 36% in 2005–2009 and again to 32% between 2009 and 2012. Since 2009, nearly all (84%) of the increase in the rate of mass loss has been due to increased surface melting and runoff.

Our findings provide observational support to recent model predictions that SMB, not discharge, is the primary driver of GrIS mass loss on decadal and greater time scales [*Goelzer et al*., 2013; *Nick et al*., 2013; *Wouters et al*., 2013]. The reasons for this are, first, that outlet glacier acceleration has not been sustained over large regions. Regionally synchronous acceleration in the southeast was short lived and acceleration of glaciers in the northwest has not been as uniform [*Joughin et al*., 2010; *McFadden et al*., 2011; *Moon et al*., 2012]. Second, even if flow speeds remain elevated, dynamic ice thinning acts to reduce discharge; an effect that becomes substantial over time periods of several years. Thus, a sustained increase in discharge is possible only if glaciers continue to accelerate. With the exception of Jakobshavn Isbræ, glacier acceleration has been brief, with glaciers accelerating over a period of days to months and then either maintaining that speed or slowing down [*Howat et al*., 2010; *Moon et al*., 2012]; as such, there are no clear regional multiyear discharge trends evident in our data set (Figure S5). Lastly, the strong negative trend in SMB has recently outpaced the increase in ice sheet discharge, particularly within the last several years (Figure 3). Additionally, on longer time scales, a more negative SMB acts to reduce discharge by removing more ice before it reaches the margin [*Goelzer et al*., 2013].

Since 2005, discharge has varied about a mean of 535 Gt/a, or approximately 110 Gt/a greater than the 1996 reference, equivalent to ~30 mm of sea level rise per century. Discharge has nearly stabilized in the southeast (Figure 1), where earlier (2000–2005) acceleration was likely driven by a synchronous retreat of grounded ice fronts off of bathymetric highs [*Howat et al*., 2008]. While the southeast glaciers may readvance and then repeat their retreat, there is no evidence that a larger, more sustained acceleration in discharge is likely from this region. As a whole, discharge from the west and northwest has been increasing by ~3 Gt/a^2 since 2000, which, if sustained would add an additional 33 mm to sea level rise by 2100. Although flow speeds along northern Greenland's ice shelf-terminating glaciers have shown negligible change since 2000 [*Moon et al*., 2012], retreat of these topographically confined ice shelves could trigger substantial acceleration and increased discharge through dynamic feedback [*Joughin et al*., 2012]. Currently, the combined discharge from the north and northeast is ~120 Gt/a, so an increase of 50%, which is much larger than has been observed for any other region, would add another 17 mm to sea level per century. Thus, assuming a continued gradual increase in discharge from the northwest, a large step increase in discharge from the north and northeast, and sustained discharge elsewhere, 21st century sea level rise from Greenland glacier discharge should not exceed 80 mm. While brief, regionally synchronous retreat and acceleration events may lead to short-term peaks in the rate of sea level rise, a greater contribution of Greenland's ice dynamics to sea level rise would take a sustained and widespread acceleration far beyond what has been observed. Our kinematic upper bound is similar to the upper bound provided by *Nick et al*. [2013] after correcting for their area-scaling approach and to other recent sea level rise projections obtained from numerical ice models [*Goelzer et al*., 2013; *Price et al*., 2011]. Given the large variability in discharge and SMB observed within the past decade and the potential for unaccounted positive feedback within the ice-climate system, however, the contribution of GrIS discharge to future sea level rise remains highly uncertain.

Acknowledgments

The work performed by E.M.E. was supported by a NASA Earth and Space Sciences Fellowship (NNX10AN76H) and I.M.H., S.J., and M.-J.N. were supported by NASA grants NNX11AR47G and NNX10AN61G. The authors acknowledge the extraordinary data collection efforts of the Center for Remote Sensing of Ice Sheet (CReSIS) and Operation IceBridge Teams.

The Editor thanks two anonymous reviewers for their assistance in evaluating this paper.

References

Ahn, Y., and I. M. Howat (2011), Efficient automated glacier surface velocity measurement from repeat images using multi-image/multichip and null exclusion feature tracking, *IEEE Trans. Geosci. Remote Sens*., *49*(8), 2838–2846.

Cuffey, K. M., and W. S. B. Paterson (2010), *The Physics of Glaciers*, 4th ed., Elsevier, Amsterdam.

Goelzer, H., P. Huybrechts, J. J. Fürst, F. M. Nick, M. L. Andersen, T. L. Edwards, X. Fettweis, A. J. Payne, and S. R. Shannon (2013), Sensitivity of Greenland ice sheet projections to model formulations, *J. Glaciol*., *59*, 216, doi:10.3189/2013JoG12J182.

Hanna, E., S. H. Mernild, J. Cappelen, and K. Steffen (2012), Recent warming in Greenland in a long-term instrumental (1881–2012) climate context: I. Evaluation of surface air temperature records, *Environ. Res. Lett*., *7*, 045,404, doi:10.1088/1748-9326/7/4/045404.

Holland, D. M., R. H. Thomas, B. de Young, M. H. Ribergaard, and B. Lyberth (2008), Acceleration of Jakobshavn Isbræ triggered by warm subsurface ocean waters, *Nat. Geosci*., *1*, doi:10.1038/ngeo316.

Howat, I. M., I. Joughin, M. Fahnestock, B. E. Smith, and T. A. Scambos (2008), Synchronous retreat and acceleration of southeast Greenland outlet glaciers 2000–06: Ice dynamics and coupling to climate, *J. Glaciol*., *54*(187), 646–660.

Howat, I. M., J. E. Box, Y. Ahn, A. Herrington, and E. M. McFadden (2010), Seasonal variability in the dynamics of marine-terminating outlet glaciers in Greenland, *J. Glaciol.*, *56*(198), 601–613.

Howat, I. M., Y. Ahn, I. Joughin, M. R. van den Broeke, J. T. M. Lenaerts, and B. Smith (2011), Mass balance of Greenland's three largest outlet glaciers, 2000–2010, *Geophys. Res. Lett.*, *38*, L12501, doi:10.1029/2011GL047565.

Joughin, I., B. E. Smith, I. M. Howat, T. Scambos, and T. Moon (2010), Greenland flow variability from ice-sheet-wide velocity mapping, *J. Glaciol.*, *56*(197), 415–430.

Joughin, I., R. B. Alley, and D. M. Holland (2012), Ice-sheet response to oceanic forcing, *Science*, *338*, 6111, doi:10.1126/science.1226481.

Khan, S. A., J. Wahr, M. Bevis, I. Velicogna, and E. Kendrick (2010), Spread of ice mass loss into northwest Greenland observed by GRACE and GPS, *Geophys. Res. Lett.*, *37*, L06501, doi:10.1029/2010GL042460.

Kjaer, K. H., et al. (2012), Aerial photographs reveal late-20th-century dynamic ice loss in northwestern Greenland, *Science*, *337*, 569, doi:10.1126/science.1220614.

Korona, J., E. Berthier, M. Bernard, F. Rémy, and E. Thouvenot (2009), SPIRIT. SPOT 5 stereoscopic survey of polar ice: Reference images and topographies during the fourth International Polar Year (2007–2009), *ISPRS J. Photogramm. Remote Sens.*, *64*, 204–212.

McFadden, E. M., I. M. Howat, I. Joughin, B. E. Smith, and Y. Ahn (2011), Changes in the dynamics of marine terminating outlet glaciers in west Greenland (2000–2009), *J. Geophys. Res.*, *116*, F02022, doi:10.1029/2010JF001757.

Moon, T., and I. Joughin (2008), Changes in ice front position on Greenland's outlet glaciers from 1992 to 2007, *J. Geophys. Res.*, *113*, F02022, doi:10.1029/2007JF000927.

Moon, T., I. Joughin, B. Smith, and I. Howat (2012), 21st-century evolution of Greenland outlet glacier velocities, *Science*, *336*, 576, doi:10.1126/science.1219985.

Nick, F. M., A. Vieli, M. L. Andersen, I. Joughin, A. Payne, T. L. Edwards, F. Pattyn, and R. S. W. van de Wal (2013), Future sea-level rise from Greenland's main outlet glaciers in a warming climate, *Nature*, *497*, doi:10.1038/nature12068.

Noh, M. J., and I. M. Howat (2013), Automated co-registration of repeat digital elevation models for surface elevations change measurement using geometric constraints, *IEEE Trans. Geosci. Remote Sens.*, 99, doi:10.1109/TGRS.2013.2258928.

Pfeffer, T., J. T. Harper, and S. O'Neel (2008), Kinematic constraints on glacier contributions to 21st-century sea-level rise, *Science*, *321*, 1340, doi:10.1126/science.1159099.

Price, S. F., A. J. Payne, I. M. Howat, and B. E. Smith (2011), Committed sea-level rise for the next century from Greenland ice sheet dynamics during the past decade, *Proc. Natl. Acad. Sci. U. S. A.*, *108*(22), 8978–8983.

Rignot, E., J. E. Box, E. Burgess, and E. Hanna (2008), Mass balance of the Greenland ice sheet from 1985 to 2007, *Geophys. Res. Lett.*, *35*, L20502, doi:10.1029/2008GL035417.

Rignot, E., I. Velicogna, M. R. van den Broeke, A. Monaghan, and J. T. M. Lenaerts (2011), Acceleration of the contribution of the Greenland and Antarctic ice sheets to sea level rise, *Geophys. Res. Lett.*, *38*, L05503, doi:10.1029/2011GL046583.

Sasgen, I., M. van den Broeke, J. L. Bamber, E. Rignot, L. S. Sorensen, B. Wouters, Z. Martinec, I. Velicogna, and S. B. Simonsen (2012), Timing and origin of recent regional ice-mass loss in Greenland, *Earth Planet. Sci. Lett.*, *333–334*, 293–303.

Seale, A., P. Christoffersen, R. I. Mugford, and M. O'Leary (2011), Ocean forcing of the Greenland ice sheet: Calving fronts and patterns of retreat identified by automatic satellite monitoring of eastern outlet glaciers, *J. Geophys. Res.*, *116*, F03013, doi:10.1029/2010JF001847.

Straneo, F., D. A. Sutherland, D. Holland, C. Gladish, G. Hamilton, H. Johnson, E. Rignot, Y. Xu, and M. Koppes (2012), Characteristics of ocean waters reaching Greenland's glaciers, *Ann. Glaciol.*, *53*, 60, doi:10.3189/2012AoG60A059.

Straneo, F., et al. (2013), Challenges to understand the dynamic response of Greenland's marine terminating glaciers to oceanic and atmospheric forcing, *Bull. Am. Meteorol. Soc.*, *94*, 1131–1144, doi:10.1175/BAMS-D-12-00100.

van Angelen, J. H., J. T. M. Lenaerts, M. R. van den Broeke, and B. Wouters (2013), Contemporary (1960–2012) evolution of the climate and surface mass balance of the Greenland ice sheet, *Surv. Geophys.*, doi:10.1007/s10712-013-9261-z.

van den Broeke, M. R., J. L. Bamber, J. Ettema, E. Rignot, E. J. O. Schrama, W. J. van de Berg, E. van Meijgaard, I. Velicogna, and B. Wouters (2009), Partitioning recent Greenland mass loss, *Science*, *326*, 984–986, doi:10.1126/science.1178176.

Walsh, K. M., I. M. Howat, Y. Ahn, and E. M. McFadden (2012), Changes in the marine-terminating glaciers of central east Greenland, 2000–2010, *Cryosphere*, *6*, doi:10.5194/tc-6-211-2012.

Wouters, B., J. L. Bamber, M. R. van den Broeke, J. T. M. Lenaerts, and I. Sasgen (2013), Limits in detecting acceleration of ice sheet mass loss due to climate variability, *Nat. Geosci.*, *6*, 613, doi:10.1038/NGEO1874.

Zwally, H. J., M. B. Giovinetto, J. Li, H. G. Cornejo, M. A. Beckley, A. C. Brenner, J. L. Saba, and D. Yi (2005), Mass changes of the Greenland and Antarctic ice sheets and shelves and contributions to sea-level rise: 1992–2002, *J. Glaciol.*, *51*(175), 509–527.